

< 7 K L V P D Q X V F U L S W Y H U V L R Q L V P D G H D Y D L O
7 K H S X E O L V K H G Y H U V L R Q L V D Y D L O D E O H Y L D K W W S V

Intracellular localization and binding partners of death associated protein kinase-related apoptosis-inducing protein kinase 1

Yuna Oue^{a,1}, Sara Murakami^{a,1}, Kinuka Isshiki^a, Akihiko Tsuji^{a,b}, and Keizo Yuasa^{a,b,*}

^a*Department of Biological Science and Technology, Tokushima University Graduate School,
Minamijosanjima, Tokushima, Japan*

^b*Department of Bioscience and Bioindustry, Tokushima University Graduate School,
Minamijosanjima, Tokushima, Japan*

¹These two authors contributed equally to this work.

*Corresponding author: kyuasa@tokushima-u.ac.jp

Abstract

Death associated protein kinase (DAPK)-related apoptosis-inducing protein kinase (DRAK)-1 is a positive apoptosis regulator. However, the molecular mechanisms underlying the DRAK1-mediated apoptotic pathway remain unclear. In this study, we demonstrated the intracellular localization and binding partners of DRAK1. In human osteosarcoma cell line U2OS cells, DRAK1 was mainly localized in the nucleus and translocated outside the nucleus through Ser³⁹⁵ phosphorylation by protein kinase C. In the nucleus, DRAK1 associated with tumor suppressor p53 and positively regulated p53 transcriptional activity in response to DNA-damaging agent cisplatin. On the other hand, DRAK1 interacted with the mitochondrial inner-membrane protein, adenine nucleotide translocase (ANT)-2, an anti-apoptotic oncoprotein, outside the nucleus. These findings suggest that DRAK1 translocates in response to stimuli and induces apoptosis through its interaction with specific binding partners, p53 and/or ANT2.

Abbreviations: DAPK, death associated protein kinase; DRAK, DAPK-related apoptosis-inducing protein kinase; ANT, adenine nucleotide translocase; VDAC, voltage-dependent anion channel; NLS, nuclear localization signal; PKC, protein kinase C; PMA, phorbol myristate acetate.

1. Introduction

Death associated protein kinase (DAPK)-related apoptosis-inducing protein kinase (DRAK) 1 is a member of the DAPK family comprising five types: DAPK1-DAPK3, DRAK1, and DRAK2 [1]. These family members have the highest homology in their Ser/Thr kinase domains at the N terminus, whereas their C-terminal regions largely differ and contain unique domains. DAPK1, which is the most studied of the family members, has a long sequence at its C terminus, comprising a calmodulin-binding domain, eight ankyrin-binding repeats, a ROC-COR domain, and a C-terminal death domain. These unique domains affect its function and localization through interaction with several protein partners [2, 3]. For example, the death domain mediates an interaction with ERK, and ERK causes an increase in DAPK1 activity by phosphorylating DAPK1 [2]. Similarly, many studies report significant relationships between specific binding proteins and the physiological functions of the other DAPK family members [1, 4]. However, although DRAK1 has been known to be exclusively localized in the nucleus and induce apoptosis [5], the molecular mechanism of the DRAK1-mediated apoptotic signaling pathway, including its binding partners, remains to be elucidated.

A recent study showed that DRAK1 is a direct target gene of tumor suppressor p53 [6]. p53 is activated by various cell stresses, such as DNA damage and activated oncogenes, thereby inducing the transcription of genes that promote cell death and growth arrest (e.g., p21, the proapoptotic protein Bax) and inhibiting the transcription of several cell-survival genes (e.g., survivin, the antiapoptotic protein Bcl-2) [7]. DRAK1 was upregulated by cisplatin, a DNA-damaging agent in various cell lines in a p53-dependent manner, and p53 directly bound to an upstream element in *DRAK1* [6]. In response to DNA damage, p53 function is regulated by phosphorylation at multiple sites. Casein kinase 2 (CK2) phosphorylates p53 at Ser³⁹², thereby enhancing DNA binding ability [8]. In addition, DAPK1 phosphorylates p53 at Ser²³ (Ser²³ in mice and Ser²⁰ in humans), and p53 transcriptionally regulates apoptosis-promoting genes, such as *Bax* [3].

Proapoptotic proteins Bax and Bad can regulate the channel activity of mitochondrial adenine nucleotide translocases (ANTs) that control the mitochondrial apoptosis pathway [9, 10]. The ANT family comprises four members, ANT1-ANT4, which are abundant in the inner mitochondrial membrane, catalyze the exchange of ADP/ATP, and regulate mitochondrial membrane permeability

together with a voltage-dependent anion channel (VDAC) [9, 11]. The expressions of ANT isoforms differ depending on the cell type. ANT1 is abundantly expressed in terminally differentiated cells, whereas ANT2 is highly expressed in undifferentiated cells with proliferating ability. Importantly, ANT2 expression is higher than that of ANT1 in several types of human cancer cells. ANT1 plays a proapoptotic role, whereas ANT2 functions as an antiapoptotic factor in cancer cells.

In this study, we investigated the mechanism of intracellular localization of DRAK1. DRAK1 was localized in the nucleus by two nuclear localization signal (NLS) sequences, and translocated outside the nucleus in response to stimuli that activate protein kinase C (PKC). Furthermore, we identified p53 and ANT2 as novel DRAK1-interacting partners. DRAK1 positively regulated p53 transcriptional activity in cisplatin-treated human osteosarcoma. These findings suggest that subcellular localization of DRAK1 through interaction with specific binding partners may be important for DRAK1 signaling.

2. Materials and methods

2.1. Antibodies

Antibody against DRAK1 was purchased from Novus Biologicals. Anti-p53, anti-phospho-p53 (Ser-392), and anti-phospho-(Ser) PKC substrate antibodies were from Cell Signaling Technology, and anti-GST and anti-glyceraldehyde-3-phosphate dehydrogenase (GAPDH) antibodies were from Wako. Anti-Strep antibody was purchased from Qiagen, and anti-FLAG antibody was from Sigma-Aldrich.

2.2. Plasmid construction

Full-length human DRAK1, DRAK2, and ANT2 cDNAs were cloned by PCR using specific primers. The DRAK1 and DRAK2 cDNAs were subcloned into a mammalian expression vector, pEXPR-IBA105 (N-terminal Strep tag) (IBA). The ANT2 cDNA was inserted in-frame into pCMV-3Tag-3A vector (C-terminal 3x FLAG tag) (Agilent Technologies). Site-directed mutagenesis was performed using the PrimeSTAR Mutagenesis Basal Kit (TaKaRa).

2.3. Cell culture, transfection, and RNA interference

U2OS, HEK293T, and COS-7 cells were cultured in DMEM supplemented with 10% FBS, 100 units/ml penicillin, and 100 µg/ml streptomycin. Transfection and RNA interference were performed using Lipofectamine 2000 (Thermo Fisher Scientific). The synthetic siRNA oligonucleotide for DRAK1 was purchased from Sigma (ID# SASI_Hs01_00136992). MISSION siRNA Universal Negative Control #1 (Sigma) was used as the negative control. Cisplatin was dissolved in 100% N,N-dimethyl formamide (DMF), and the final concentration of DMF in the culture medium was 0.1%.

2.4. Immunofluorescence analysis.

Immunofluorescence analysis was performed as previously described [12]. In brief, U2OS cells were transfected with various expression plasmids in the presence or absence of mitochondria-targeted mKeima-Red expression plasmid, pMT-mKeima-Red (MBL). After 24 hours, cells were fixed,

permeabilized, and then blocked in 5% BSA. Cells were incubated with anti-Strep or anti-GST antibodies, followed by incubation with anti-IgG directly conjugated to AlexaFluor 488 or 555 (Thermo Fisher Scientific). Fluorescent images were obtained using an IN Cell Analyzer 6000 system (GE Healthcare).

2.5. Protein identification by MALDI-TOF MS

HEK293T cells were transfected with Strep-DRAK1 or DRAK2 expression plasmids. After 24 hours, the cells were scraped in cell lysis buffer (20 mM Tris-HCl, pH 7.5, 150 mM NaCl, 0.5% Nonidet P-40, 1 mM EDTA, 10 µg/ml leupeptin, and 10 µg/ml aprotinin). After centrifugation, the supernatants were incubated with Strep-Tactin Sepharose (IBA). After the beads were washed, the bound proteins were eluted with SDS-loading buffer and resolved by 12% SDS-PAGE, followed by silver staining. The subsequent protocol has previously been described [4].

2.6. Pull-down assay

HEK293T and COS-7 cells transfected with N-terminal Strep-tagged or GST-fused DRAK1 together with C-terminal FLAG-tagged ANT2 were scraped in lysis buffer, and cell lysates were incubated with Strep-Tactin or Glutathione Sepharose (GE Healthcare) overnight at 4°C by rotation. The bound proteins were analyzed by immunoblot analysis using anti-FLAG antibody.

2.7. Luciferase reporter assay

U2OS cells were plated at a density of 2×10^4 cells in a 24-well plate. After 24 hours, the cells were transfected with negative control siRNA or DRAK1 siRNA. Six hours later, cells were transfected with pGL4.38 [luc2P/p53 RE/Hygro] (Promega), which contains two tandem repeats of a p53 response element, together with pCMV-β-gal for 24 hours. After treatment with 30 µM cisplatin for 24 hours, the cells were lysed with cell culture lysis reagent (Promega) and subjected to luciferase reporter assay. Luciferase and β-galactosidase activities were measured as previously described [13].

2.8. Statistical analysis

All experiments were performed multiple times to confirm their reproducibility. One representative set of data was shown in the figures. The results were quantified using Image J software (NIH). Data were expressed as the mean \pm standard error, and statistical analysis was performed by one-way analysis of variance (ANOVA) with Tukey's multiple comparison test using GraphPad Prism (GraphPad Software).

3. Results

3.1. Subcellular localization of DRAK1 in U2OS cells

A previous study demonstrated that DRAK1 is exclusively localized in the nucleus of COS-7 cells [5]. However, a recent report showed that subcellular localization of DRAK1 is dependent on cell type, and that DRAK1 is localized in the cytoplasm but not the nucleus in head and neck squamous cell carcinoma cell lines [14]. Therefore, we first examined the subcellular localization of the N-terminal Strep-tagged DRAK1 wild type (Strep-DRAK1-WT) in human osteosarcoma cell line U2OS cells. Immunostaining analysis revealed that Strep-DRAK1-WT was localized mainly in the nucleus and only slightly localized in the cytoplasm in U2OS cells (Fig. 1B (i)). Similar results were obtained in HeLa cells (data not shown). Since DRAK1 was localized mainly in the nucleus, we examined whether the NLS sequence exists in the DRAK1 amino acid sequence. DRAK1 contains two patches of basic residues (Arg or Lys), one in the catalytic domain (⁹³RKRRKG) and one near the C terminus (³⁹⁵SKRFFK) (Fig. 1A). Thus, we constructed two mutants, DRAK1-K94A/R95A/R96A and DRAK1-K396A/R397A, in which each of the putative NLS sites was replaced by Ala, and examined their subcellular localization. As shown in Figs. 1B (ii) and (iii), the mutants were scarcely observed in the nucleus and both localized in the cytoplasm, considering that these sequences are required for nuclear localization. The sequence near the C terminus (³⁹⁵SKRFFK) matched the consensus phosphorylation motif for PKC (*p*S-X-(R/K)). Because of the possibility that Ser³⁹⁵ immediately adjacent to NLS at the C terminus might mask its function when phosphorylated, we created the phosphomimic mutant DRAK1-S395D, in which Ser³⁹⁵ was replaced with Asp, and examined its intracellular localization. DRAK1-S395D was also found in the cytoplasm but not in the nucleus (Fig. 1B (iv)). Furthermore, we investigated whether two PKC activators, phorbol myristate acetate (PMA) and 1-oleoyl-2-acetyl-sn-glycerol (OAG), influence DRAK1's subcellular localization. U2OS cells expressing Strep-DRAK1-WT or -S395A were treated with either PMA or OAG. Both PKC activators induced the translocation of Strep-DRAK1-WT into the cytoplasm, including the mitochondria, and exhibited colocalization with a mitochondrial marker (Fig. 1C, data not shown). On the contrary, phospho-null mutant S395A, in which the putative PKC phosphorylation site was replaced by Ala, failed to translocate into the cytoplasm in response to PKC stimulation. In addition,

we examined the phosphorylation of Strep-DRAK1 in U2OS cells treated with PMA. After stimulation with PMA, the cell lysates were subjected to a Strep pull-down assay and immunoblotting with anti-phospho-(Ser) PKC substrate antibody. As shown in Fig. 1D, DRAK1-WT was phosphorylated after PMA stimulation, whereas DRAK1-S395A was not. These results suggest that DRAK1 is normally localized primarily in the nucleus, but it translocates outside the nucleus after stimulation accompanied by PKC activation.

3.2. Regulation of p53 transcriptional activity by DRAK1 in cisplatin-treated U2OS cells

A previous study showed that the expression of DRAK1 is induced by cisplatin, a DNA-damaging agent that induces cell death primarily by apoptosis, in testicular cancer cells in a p53-dependent manner [6]. Cisplatin has also induced DRAK1 expression in U2OS cells that express endogenous wild-type p53. On the other hand, p53 activity is shown to be regulated by phosphorylation at multiple sites, including Ser³⁹² [7]. Because Strep-DRAK1-WT and FLAG-p53 were colocalized in the nucleus (Fig. 2A), we hypothesized that DRAK1 might also regulate p53 transcriptional activity. To test this hypothesis, we first examined whether DRAK1 interacts with p53. U2OS cells were transfected with Strep-DRAK1-WT, and the cell lysates were subjected to the pull-down assay and immunoblotting with an anti-p53 antibody. Although p53 was endogenously expressed in U2OS cells, no interaction between DRAK1-WT and p53 was observed under normal conditions (Fig. 2B). However, when the cells were treated with cisplatin, the level of p53 protein was increased, and p53 accordingly interacted with DRAK1-WT. Conversely, p53 did not bind to the phosphomimic mutant S395D. Because DRAK2 has an amino acid sequence highly similar to that of DRAK1 and is also localized in the nucleus [15], we investigated whether it could also interact with p53. Although DRAK1 bound to p53 in cisplatin-treated cells, DRAK2 did not (Fig. 2C). These results suggest that DRAK1 specifically interacts with p53 in the nucleus in response to DNA damage.

We also examined the endogenous expression of DRAK1 in cisplatin-treated U2OS cells. DRAK1 was not normally expressed in U2OS cells, but cisplatin dose-dependently upregulated DRAK1 expression (Fig. 2D). Importantly, the phosphorylation of p53 at Ser³⁹², which is known to enhance sequence-specific DNA binding [8], was significantly increased after treatment with 30 μ M

cisplatin. Thus, we assessed whether DRAK1 affects the phosphorylation of p53 at Ser³⁹² by knockdown analysis using siRNA. DRAK1 expression induced by cisplatin was efficiently reduced by DRAK1 siRNA (Fig. 2D). Although the overall amount of p53 remained the same, DRAK1 siRNA significantly reduced the level of p53 phosphorylation at Ser³⁹². Because Ser³⁹² phosphorylation enhances DNA binding ability, we subsequently examined the effect of DRAK1 on p53 transcriptional activity. U2OS cells were transfected with the luciferase reporter construct containing two copies of the p53-responsive element. After treatment with cisplatin, luciferase and β -galactosidase activities were determined. Cisplatin increased p53 promoter activity, and which was significantly reduced by DRAK1 knockdown (Fig. 2E). A similar result was obtained using another DNA-damaging agent, etoposide (data not shown). These results demonstrated that DRAK1 positively regulates p53 transcriptional activity.

3.3. DRAK1 interacts with ANT2 outside the nucleus

We then attempted to identify novel DRAK1 binding partners using a combination of pull-down assays and mass spectrometry, which is useful for identifying interacting proteins [4]. Strep-DRAK1 or -DRAK2 was expressed in HEK293T cells, and the Strep pull-down proteins were resolved by SDS-PAGE followed by silver staining. To exclude non-specific binding, lysates of the cells transfected with an empty Strep vector were used as the negative controls. Fig. 3A shows a typical gel result. The specific protein bands at 31 and 60 kDa were found in the lysates of cells transfected with Strep-DRAK1. Because the band at 60 kDa was close to the molecular mass of Strep-DRAK1 protein, the band at 31 kDa was excised and analyzed by MALDI-TOF MS after in-gel tryptic digestion. The analysis showed that the 31-kDa protein was ANT2 (Fig. 3B). To confirm the interaction between DRAK1 and ANT2, we performed a Strep pull-down assay using lysates from cells expressing Strep-DRAK1 and the C-terminal FLAG-tagged ANT2 (ANT2-FLAG). As shown in Fig. 3C, Strep-DRAK1-WT specifically interacted with ANT2-FLAG. Because ANT2 localizes in the mitochondria, we examined the ability of DRAK1 mutants that mainly localized in the cytoplasm to bind to ANT2. Both S395D and K396A/R397A mutants, which localized in the cytoplasm, including the mitochondria, showed stronger interactions with ANT2 compared to DRAK1-WT (Fig. 3C). To

identify the regions of DRAK1 that are responsible for binding to ANT2, we produced various truncated mutants of DRAK1 as GST fusion proteins (Fig. 3D), and performed GST pull-down assays. We confirmed that GST-fused full-length DRAK1 (GST-DRAK1-WT) interacted with ANT2-FLAG. The catalytic domain (amino acids 61-321) of DRAK1 (GST-DRAK1-CD) was required for binding to ANT2. Notably, the binding of GST-DRAK1 to ANT2-FLAG was relatively stronger than that of Strep-DRAK1. Therefore, we investigated the subcellular localization of GST-DRAK1. Although Strep-DRAK1-WT was localized in the nucleus, GST-DRAK1-WT was localized outside the nucleus similar to Strep-DRAK1-K396A/R397A (Fig. 3E), resulting in stronger interaction with mitochondrial ANT2. Finally, we examined whether DRAK1 indirectly binds to ANT2 through an interaction with mitochondrial outer-membrane protein VDAC, because ANT2 is a mitochondrial inner-membrane protein. As shown in Fig. 3F, Strep-DRAK1 failed to interact with VDAC, although it interacted with endogenous ANT2. These results suggest that DRAK1 might directly interact with ANT2 at the mitochondria.

4. Discussion

The dynamic subcellular localization of many signaling molecules plays a pivotal role in their function. In the present study, we demonstrated that DRAK1 was exclusively localized in the nucleus and translocated into the cytosol, including the mitochondria, in response to PKC activation in U2OS cells (Fig. 4). DRAK1 contains two NLS sequences, one in the catalytic domain (⁹³RKRRKG) and one near the C terminus (³⁹⁵SKRFFK). A previous study reveals that DRAK2 also localizes in the nucleus through NLS (³⁵⁰SKRFR in rat) in its C terminus, and PKC induces the translocation of DRAK2 into the cytoplasm by phosphorylating DRAK2 at Ser³⁵⁰ [15]. DRAK2 has an amino acid sequence highly similar to that of DRAK1 (52% identity, 83% similarity). However, although DRAK1 interacted with p53, DRAK2 did not. DRAK1 contains a proline-rich region (³⁰PCRPPPPP) in the N terminus, although its role remains unclear. Generally, the proline-rich region is involved in protein-protein interactions [16]. For example, Src homology (SH)-3 and WW domains associate with specific proline-rich sequences. p53 also has the proline-rich domain, which contains 14 prolines and 5 repeats of the PXXP motif, a binding site for SH3 domains [16]. It has also been shown that the proline-rich domain of p53 is necessary for apoptosis and efficient growth suppression elicited by p53 [17]. Taken together, DRAK1 might directly or indirectly interact with p53 through the proline-rich region.

We also showed that cisplatin induced the expression of both p53 and DRAK1 in U2OS cells. Apoptosis-related genes, such as *Bax*, are transcriptionally induced by p53, which is activated by DNA damage and oncogenes. A previous study observed that p53 directly binds to an upstream element in *DRAK1* and induces DRAK1 expression [6]. More importantly, cisplatin-induced phosphorylation of p53 at Ser³⁹² was reduced by DRAK1 knockdown, although the total amount of p53 did not change. Furthermore, cisplatin-induced p53 promoter activity was decreased by DRAK1 knockdown. These results suggested that DRAK1 might modulate the transcriptional activity of p53 and p53-mediated apoptosis through a positive-feedback loop. It is still unknown whether DRAK1 directly phosphorylates p53 at Ser³⁹², the site that is directly phosphorylated by a few kinases, including CK2 [8]. The amino acid sequence surrounding Ser³⁹² of p53 (KTEGPD³⁹²SD) does not conform to the consensus phosphorylation sequence for the DAPK family members. However, it is possible that DRAK1 phosphorylates p53 at Thr¹⁸ and Ser²⁰ (LSQE¹⁸TF²⁰SDL), although neither site conforms to

the consensus phosphorylation sequence [18]. Further studies will reveal whether DRAK1 could directly or indirectly activate p53.

Furthermore, we identified ANT2 as a DRAK1 binding partner. Mitochondrial inner-membrane protein ANT2 regulates mitochondrial membrane permeability together with mitochondrial outer-membrane protein VDAC. Although we hypothesized that DRAK1 indirectly binds to ANT2 through an interaction with VDAC, we found that DRAK1 did not associate with VDAC, suggesting that DRAK1 might translocate across the mitochondrial outer membrane and interact directly with ANT2. ANT1 and ANT3 transport ATP from the mitochondria into the cytoplasm, whereas ANT2, which is highly expressed in tumor cells, could import glycolytically produced ATP into the mitochondrial matrix [19]. It has been shown that ANT2 knockdown in human breast cancer cells induces apoptosis and inhibits tumor growth through the upregulation of proapoptotic protein Bax and the downregulation of antiapoptotic protein Bcl-xL [20]. These suggest that ANT2 exhibits an antiapoptotic function in cancer cells by inhibiting mitochondrial membrane permeabilization [19, 20]. Because ANT1-mediated ADP/ATP exchange is regulated by the Src-mediated tyrosine phosphorylation of ANT1 [21], DRAK1 might induce apoptosis by regulating ANT2 activity through its interaction and phosphorylation. On the other hand, p53 also translocates into the mitochondria in response to cell-death stimuli [22]. Translocated mitochondrial p53 can induce permeabilization of the outer mitochondrial membrane by forming complexes with the protective Bcl-xL and Bcl-2, resulting in cytochrome c release into the cytoplasm. We still need to elucidate how DRAK1 translocates across the mitochondrial outer membrane and binds to ANT2, and determine the physiological significance of the interaction between DRAK1 and ANT2.

In conclusion, we demonstrated that DRAK1 was localized mainly in the nucleus and translocated outside the nucleus in response to PKC activation. In the nucleus, DRAK1 bound to p53 and positively controlled its transcriptional activity, suggesting that these two proteins have the potential to coordinate signaling through positive-feedback regulation. In the mitochondria, DRAK1 interacted with ANT2. Because ANT2 acts as an antiapoptotic oncoprotein, DRAK1 might be involved in the regulation of apoptosis through its interaction with ANT2. These findings contribute to the elucidation of the apoptotic signaling transduction pathway and to the development of more

effective anticancer agents. Further studies could reveal the mechanism by which apoptosis is regulated by the interaction between DRAK1 and p53 and/or ANT2.

Acknowledgements

The authors thank Ms. Yuka Sasaki and Mr. Tomohiro Komai for their technical assistance. This study was supported in part by Grant-in-Aid for Japan Society for the Promotion of Science Fellows (K. Isshiki) and by a grant from the Awa Bank Science and Culture Foundation of Tokushima (K. Yuasa).

References

- [1] R. Shiloh, S. Bialik, A. Kimchi, The DAPK family: a structure-function analysis. *Apoptosis* 19(2014)286-297.
- [2] C.H. Chen, W.J. Wang, J.C. Kuo, H.C. Tsai, J.R. Lin, Z.F. Chang, R.H. Chen, Bidirectional signals transduced by DAPK-ERK interaction promote the apoptotic effect of DAPK. *EMBO J.* 24(2005)294-304.
- [3] L. Pei, Y. Shang, H. Jin, S. Wang, N. Wei, H. Yan, Y. Wu, C. Yao, X. Wang, L.Q. Zhu, Y. Lu, DAPK1-p53 interaction converges necrotic and apoptotic pathways of ischemic neuronal death. *J.Neurosci.* 34(2014)6546-6556.
- [4] K. Isshiki, S. Matsuda, A. Tsuji, K. Yuasa, cGMP-dependent protein kinase I promotes cell apoptosis through hyperactivation of death-associated protein kinase 2. *Biochem.Biophys.Res.Comm.* 422(2012)280-284.
- [5] H. Sanjo, T. Kawai, S. Akira, DRAKs, novel serine/threonine kinases related to death-associated protein kinase that trigger apoptosis. *J.Biol.Chem.* 273(1998)29066-29071.
- [6] P. Mao, M.P. Hever, L.M. Niemaszyk, J.M. Haghkerdar, E.G. Yanco, D. Desai, M.J. Beyrouthy, J.S. Kerley-Hamilton, S.J. Freemantle, M.J. Spinella, Serine/threonine kinase 17A is a novel p53 target gene and modulator of cisplatin toxicity and reactive oxygen species in testicular cancer cells. *J.Biol.Chem.* 286(2011)19381-19391.
- [7] D.W. Meek, Regulation of the p53 response and its relationship to cancer. *Biochem.J.* 469(2015)325-346.
- [8] D.M. Keller, X. Zeng, Y. Wang, Q.H. Zhang, M. Kapoor, H. Shu, R. Goodman, G. Lozano, Y. Zhao, H. Lu, A DNA damage-induced p53 serine 392 kinase complex contains CK2, hSpt16, and SSRP1. *Mol.Cell* 7(2001)283-292.
- [9] A. Chevrollier, D. Loiseau, P. Reynier, G. Stepien G, Adenine nucleotide translocase 2 is a key mitochondrial protein in cancer metabolism. *Biochim.Biophys.Acta* 1807(2011)562-567.
- [10] A.S. Belzacq, H.L. Vieira, F. Verrier, G. Vandecasteele, I. Cohen, M.C. Prévost, E. Larquet, F. Pariselli, P.X. Petit, A. Kahn, R. Rizzuto, C. Brenner, G. Kroemer, Bcl-2 and Bax modulate adenine nucleotide translocase activity. *Cancer Res.* 63(2003)541-546.

- [11] A. Doerner, M. Pauschinger, A. Badorff, M. Noutsias, S. Giessen, K. Schulze, J. Bilger, U. Rauch, H.P. Schultheiss, Tissue-specific transcription pattern of the adenine nucleotide translocase isoforms in humans. *FEBS Lett.* 414(1997)258-262.
- [12] S. Matsuda, K. Kawamoto, K. Miyamoto, A. Tsuji, K. Yuasa, PCTK3/CDK18 regulates cell migration and adhesion by negatively modulating FAK activity. *Sci.Rep.* 7(2017)45545.
- [13] K. Yuasa, S. Uehara, M. Nagahama, A. Tsuji, Transcriptional regulation of cGMP-dependent protein kinase II (cGK-II) in chondrocytes. *Biosci.Biotechnol.Biochem.* 74(2010)44-49.
- [14] Y. Park, W. Kim, J.M. Lee, J. Park, J.K. Cho, K. Pang, J. Lee, D. Kim, S.W. Park, K.M. Yang, S.J. Kim, Cytoplasmic DRAK1 overexpressed in head and neck cancers inhibits TGF- β 1 tumor suppressor activity by binding to Smad3 to interrupt its complex formation with Smad4. *Oncogene* 34(2015)5037-5045.
- [15] H. Kuwahara, M. Nishizaki, H. Kanazawa, Nuclear localization signal and phosphorylation of serine350 specify intracellular localization of DRAK2. *J.Biochem.* 143(2008)349-358.
- [16] B.K. Kay, M.P. Williamson, M. Sudol, The importance of being proline: the interaction of proline-rich motifs in signaling proteins with their cognate domains. *FASEB J.* 14(2000)231-241.
- [17] C. Venot, M. Maratrat, C. Dureuil, E. Conseiller, L. Bracco, L. Debussche, The requirement for the p53 proline-rich functional domain for mediation of apoptosis is correlated with specific PIG3 gene transactivation and with transcriptional repression. *EMBO J.* 17(1998)4668-4679.
- [18] A.L. Craig, J.A. Chrystal, J.A. Fraser, N. Sphyris, Y. Lin, B.J. Harrison, M.T. Scott, I. Dornreiter, T.R. Hupp, The MDM2 ubiquitination signal in the DNA-binding domain of p53 forms a docking site for calcium calmodulin kinase superfamily members. *Mol.Cell.Biol.* 27(2007)3542-3555.
- [19] A. Chevrollier, D. Loiseau, B. Chabi, G. Renier, O. Douay, Y. Malthiery, G. Stepien, ANT2 isoform required for cancer cell glycolysis. *J.Bioenerg.Biomembr.* 37(2005)307-316.
- [20] J.Y. Jang, Y. Choi, Y.K. Jeon, C.W. Kim, Suppression of adenine nucleotide translocase-2 by vector-based siRNA in human breast cancer cells induces apoptosis and inhibits tumor growth in vitro and in vivo. *Breast Cancer Res.* 10(2008)R11
- [21] J. Feng, E. Lucchinetti, G. Enkavi, Y. Wang, P. Gehrig, B. Roschitzki, M.C. Schaub, E. Tajkhorshid, K. Zaugg, M. Zaugg, Tyrosine phosphorylation by Src within the cavity of the

adenine nucleotide translocase 1 regulates ADP/ATP exchange in mitochondria. *Am.J.Physiol.* 298(2010)C740-748.

[22] S. Erster, M. Mihar, R.H. Kim, O. Petrenko, U.M. Moll, In vivo mitochondrial p53 translocation triggers a rapid first wave of cell death in response to DNA damage that can precede p53 target gene activation. *Mol.Cell.Biol.* 24(2004)6728-6741.

Figure legends

Fig. 1. Subcellular localization of DRAK1 in U2OS cells. (A) Schematic representations of DRAK1. (B and C) U2OS cells were transfected with Strep-DRAK1-WT or its mutants in the presence or absence of mitochondria-targeted mKeima-Red expression plasmid (*mito-Red*). After 20 hours, cells were serum-starved for 5 hours and treated with 100 nM PMA or DMSO for 60 min (C). After fix and permeabilization, cells were incubated with anti-Strep antibody, followed by AlexaFluor 488-conjugated secondary antibody. All images were obtained using 40× objective lens of IN Cell Analyzer 6000. (D) U2OS cells expressing Strep-DRAK1-WT or -S395A were stimulated with 50 nM PMA for 60 min. Cell lysates were pulled down with Strep-Tactin Sepharose, followed by immunoblotting with anti-phospho-(Ser) PKC substrate antibody. All experiments were performed multiple times with similar results.

Fig. 2. Regulation of p53 activity by DRAK1 in cisplatin-treated U2OS cells. (A) U2OS cells were transfected with Strep-DRAK1-WT and FLAG-p53. After fix, cells were incubated with anti-Strep antibody and anti-FLAG antibody, followed by AlexaFluor 488 and 555-conjugated secondary antibodies. (B) U2OS cells transfected with Strep-DRAK1-WT or -S395D were treated with 30 μ M cisplatin or DMF for 24 hours. The cell lysates were subjected to the pull-down assay and immunoblotting with an anti-p53 antibody. (C) U2OS cells expressing Strep-DRAK1 or Strep-DRAK2 were treated with 30 μ M cisplatin for 24 hours. The cell lysates were used in pull-down assay. (D) U2OS cells were transfected with negative control siRNA (*siNC*) or DRAK1 siRNA (*siDRAK1*). After 24 hours, the cells were treated with 0, 10, or 30 μ M cisplatin for 24 hours. The cell lysates were subjected to immunoblot analysis. The levels of total p53 and phosphorylated p53 were normalized to GAPDH levels. The values obtained from the negative control siRNA-transfected cells treated with 30 μ M cisplatin were taken as 100%. (E) U2OS cells were transfected with negative control siRNA or DRAK1 siRNA, followed by transfection with the p53-responsive reporter plasmid and pCMV- β -gal. The cells were treated with 30 μ M cisplatin for 24 hours. After harvest, luciferase and β -galactosidase activities were measured, and the luciferase activity was normalized to the β -galactosidase activity. All data are presented as the mean \pm standard error derived from at least three

independent experiments, and statistical analysis was performed by one-way ANOVA with Tukey's multiple comparison test.

Fig. 3. DRAK1 interacts with ANT2 outside the nucleus. (A) HEK293T cells transfected with Strep empty vector, Strep-DRAK1, or Strep-DRAK2, were scraped and used in a Strep pull-down assay. The bound proteins were resolved by SDS-PAGE, followed by silver staining. (B) Tryptic fragments of human ANT2 identified by MALDI-TOF MS. (C) HEK293T cells were transfected with Strep-DRAK1-WT or its mutants (Strep-DRAK1-S395D and -K396A/R397A) together with ANT2-FLAG. The cell lysates were used in a Strep pull-down assay. (D) HEK293T cells were transfected with GST-DRAK1-WT or its mutants (DRAK1-N, - Δ C, and -CD) together with ANT2-FLAG. The cell lysates were pulled down with glutathione Sepharose and analyzed by immunoblotting. (E) U2OS cells were transfected with Strep-tagged or GST-tagged DRAK1-WT and its mutant (DRAK1-K396A/R397A). Cells were fixed and stained with antibodies against Strep and GST, followed with AlexaFluor 488-conjugated secondary antibody. (F) HEK293T cells were transfected with Strep-DRAK1-WT or its mutants. The cell lysates were used in a Strep pull-down assay. All experiments were performed multiple times with similar results.

Fig. 4. Proposed model of the DRAK1 signaling pathway. *p53 RE*, p53-responsive element.

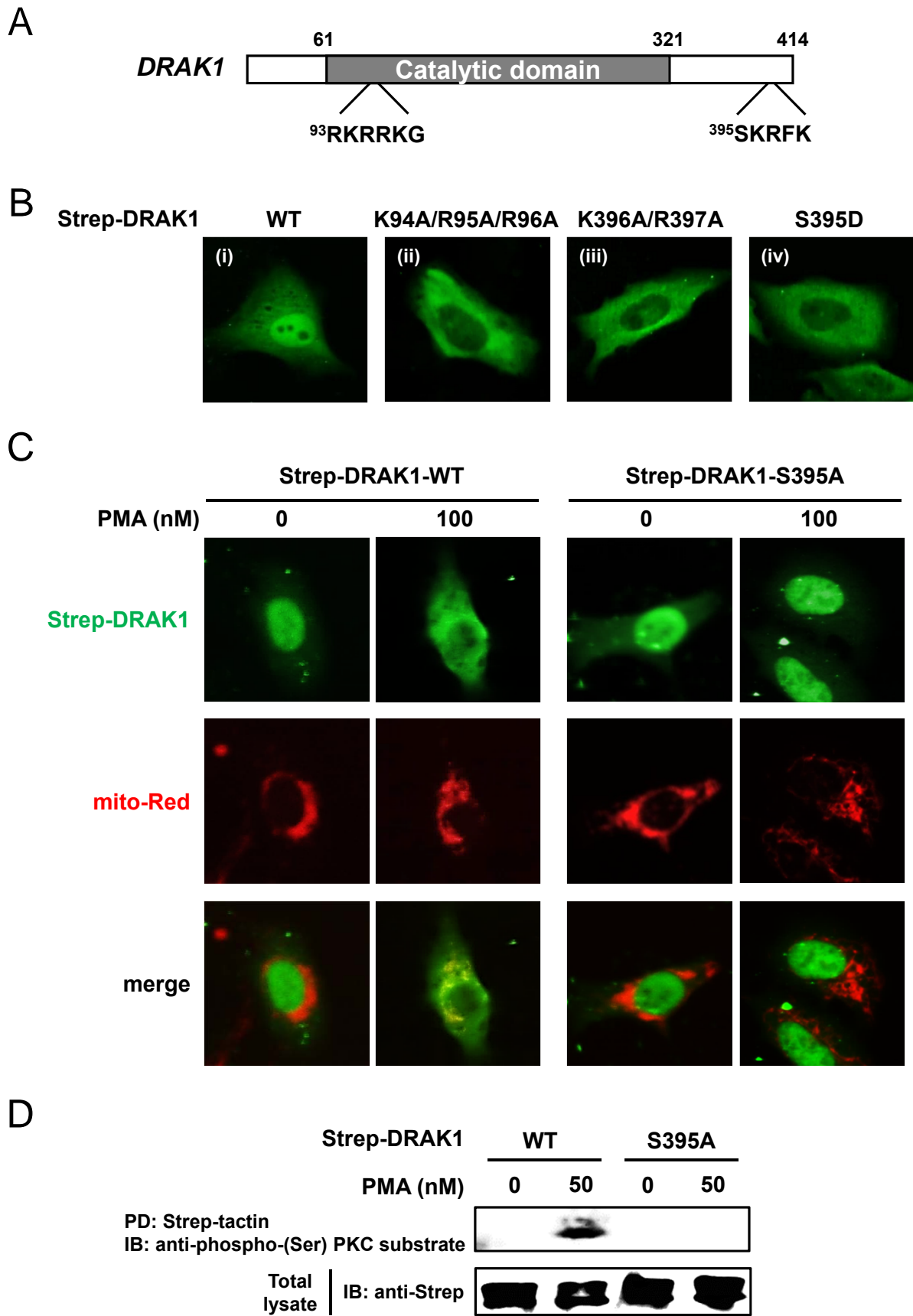


Fig. 1. Oue et al. (2018)

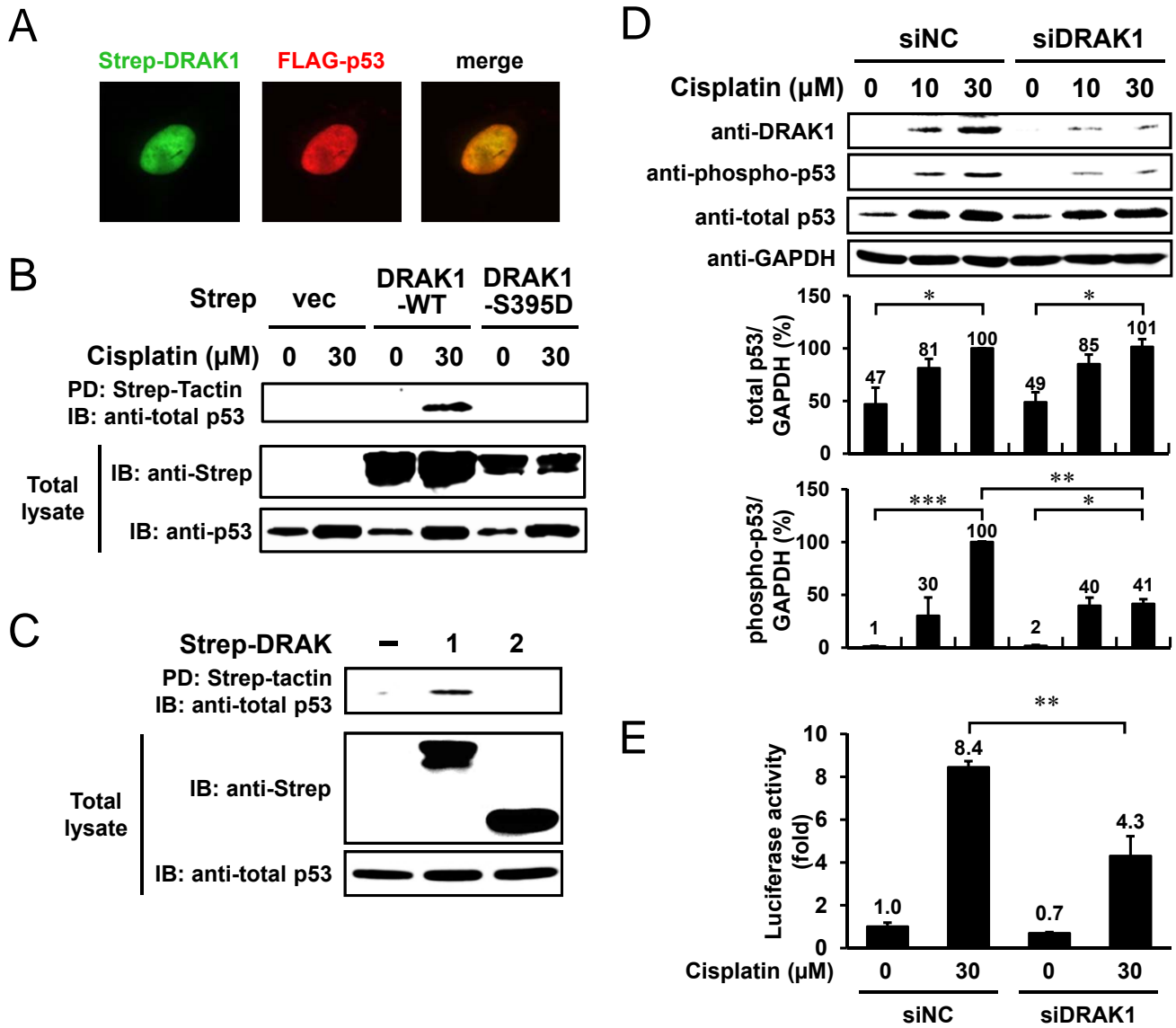


Fig. 2. Oue et al. (2018)

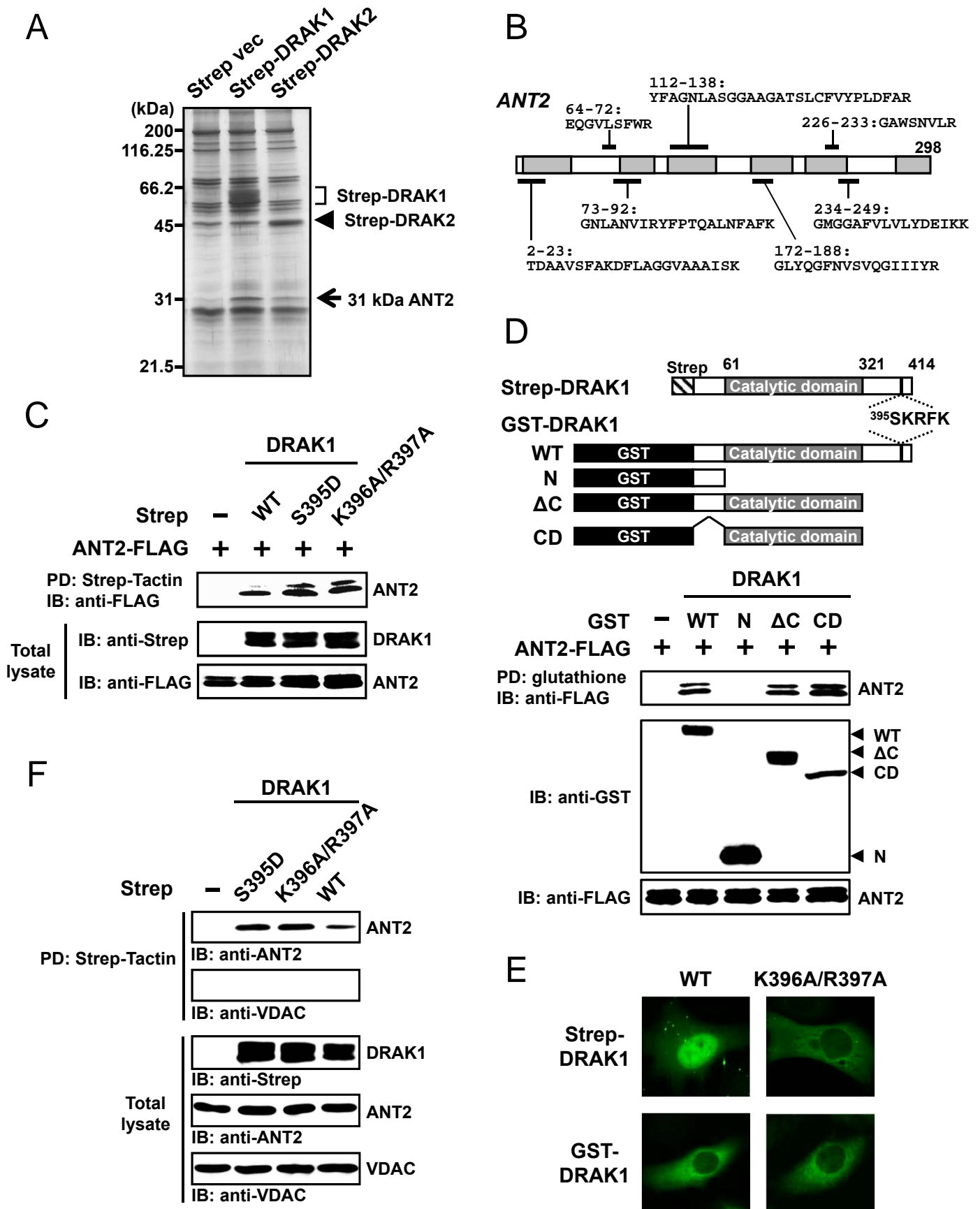


Fig. 3. Oue et al. (2018)

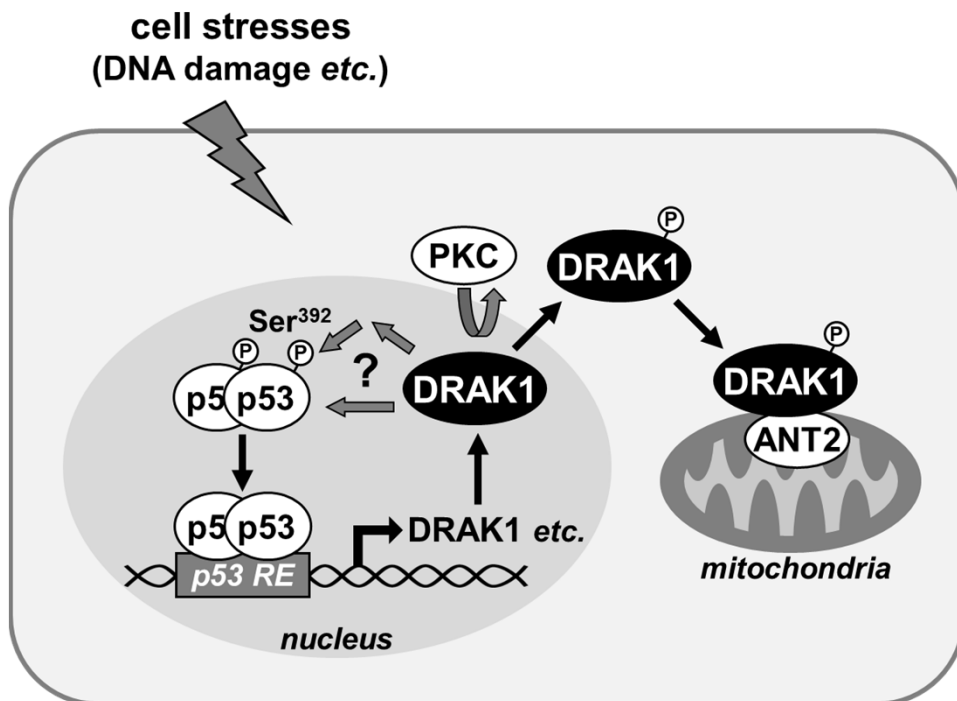


Fig. 4. Oue et al. (2018)